Composites Science and Technology 119 (2015) 26–33

Contents lists available at ScienceDirect

Composites Science and Technology

journal homepage: http://www.elsevier.com/locate/compscitech

Mechanical properties of carbon fiber composite octet-truss lattice structures

Liang Dong*, Haydn Wadley

Department of Materials Science and Engineering, University of Virginia, Charlottesville, VA 22903, United States

ARTICLE INFO

Article history:
Received 16 June 2015
Received in revised form
1 September 2015
Accepted 22 September 2015
Available online 28 September 2015

Keywords:
Octet-truss lattice
Elastic stiffness
Strength
Carbon fiber composite

ABSTRACT

Octet-truss lattice structures have been made from balanced [0/90] carbon fiber reinforced polymer (CFRP) laminates using a simple snap-fit method. The lattice structures moduli and strengths have been measured during [001] and [100] directions free compressions as a function of the lattice relative density. Core failure occurred by either (i) Euler buckling ($\bar{\rho} < 5\%$) or (ii) delamination dominated failure ($\bar{\rho} > 5\%$) of the struts. The measurements are shown to be well predicted by micromechanics models of these composite strut failure modes. Snap-fit CFRP octet-truss lattice structures are found to exhibit mechanical properties competitive with other cellular materials and topologies. Their isotropic response may provide new opportunities for ultra-lightweight multiaxial loaded structures.

1. Introduction

The octet-truss lattice structure first proposed by Fuller [1] provides a method for filling 3-D space with a structurally efficient truss structure of an arbitrary cell size. This stretch-dominated structure has a high nodal connectivity of 12 [2], and an almost isotropic yield surface [3]. Recent alloy casting approaches have demonstrated the possibility of making octet-truss lattices with strut lengths in the 5–10 mm range [3]. Wrought titanium alloy octet-truss lattices have also been recently fabricated [4] while self-propagating waveguide or laser based stereolithographic methods, when combined with electroless nickel plating or vapor deposition, have enabled fabrication of micrometer scale structures [5–7].

Material property charts provide a useful way to compare the mechanical properties of these low density materials. Fig. 1 compares the density dependent moduli and strengths of compressively loaded polymer and metal foams and lattice structures made by investment cast of aluminum [3] and titanium alloys [8,9], electrodeposition of Ni–7P [5,6], carbon fiber composites via a reversible assembly technique [10], photosensitive HDDA polymers [6], and by the vapor deposition of alumina [6,7]. Recently reported Ti–6Al–4V octet-truss lattice structures [4], balsa wood [11], polymer [12] and metallic [13] syntactic foams are also included in these Ashby maps. Foams have a low nodal connectivity, and are bending governed structures, and therefore compliant and weaker than lattice topology counterparts. When made from high specific strength materials, the octet-truss lattice is a highly weight efficient, multiaxial stress supporting structure, with a stiffness and strength that scale linearly with the lattice relative density, $\bar{\rho}$ (the density of the lattice structure divided by that of the material from which it was made) [14] if the struts failed by plastic deformation.

Carbon fiber composites (CFRP) have a high specific strength and stiffness and is therefore a promising material for making stiff and potentially strong cellular structures. Here, we explore the application of a simple "snap-fit" assembly method [15] for fabricating octet-truss cellular materials from CFRP laminate materials. The [001] and [100] directions compressive properties of the octet-truss lattices have been characterized as a function of the lattice relative density and compared to micromechanical predictions.

2. Lattice fabrication and laminate material properties

The as-received [0/90] CFRP laminate sheets (McMaster-Carr) have a thickness t = 1.59 mm, and a density 1.44 Mg/m^3. They contained 55 vol% 228 GPa carbon fiber in a vinyl ester matrix. The laminate was comprised of 7 plies. The 2 surface plies were made from plain weave fabrics while the 5 interior plies were unidirectional and laid up in a $[0/90]_5$ arrangement (Supplementary information S.1). The laminate sheets were fabricated in such a

* Corresponding author.
E-mail address: ld5fy@virginia.edu (L. Dong).

http://dx.doi.org/10.1016/j.compscitech.2015.09.022
0266-3538/

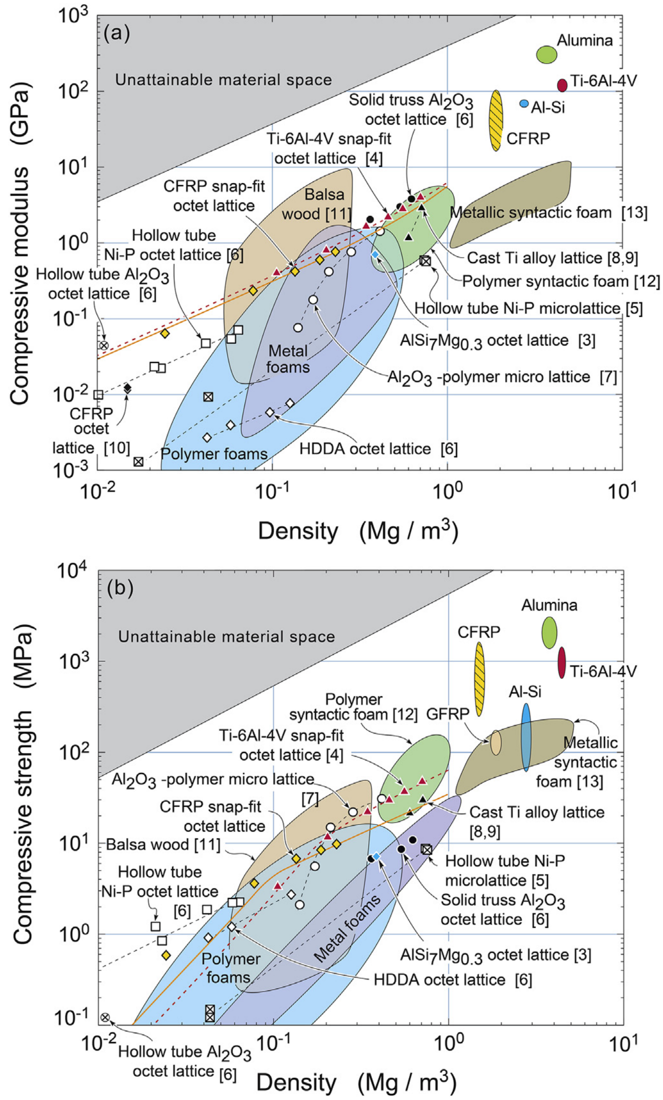

Fig. 1. Material property charts showing (a) stiffness and (b) strength versus density for octet-truss lattices and several other topology cellular structures.

way that the volume fraction of fibers along the laminate longitudinal direction (parallel to 0° unidirectional plies) is equivalent to that of fibers along the laminate transverse direction (parallel to 90° unidirectional plies). However, the 0° unidirectional plies had a volume approximately 1.5 times that of the 90° unidirectional plies. This volume difference was compensated by different volumes of warp and weft tows in the surface plies. Laminate sheets with woven plies on the outer surfaces were selected for the present study since they have better toughness and impact strength, and are less susceptible to delamination during machining operations such as drilling, side milling and slotting [16]. Thus, the use of laminate sheets with woven surface plies was driven by a manufacturing constraint: the need to avoid delamination failures during fabrication and assembly of the lattice structures.

The CFRP octet-truss lattice structures were fabricated from the as-received [0/90] CFRP laminate sheets in a three step process, Fig. 2. The pyramidal truss row patterns, Fig. 2(a), and intermediate faces, Fig. 2(c), were water jet and CNC mill cut separately from the laminate sheets so that half the fibers were parallel to the struts axes. Note that the strut axis was chosen to be parallel either to the laminates longitudinal or transverse directions. We subsequently use “longitudinal strut” and “transverse strut” to denote octet struts with axes parallel to the longitudinal and transverse directions of the laminate sheet from which they were cut. Rows of pyramidal trusses were collinearly aligned and a second collinear array attached to their top, forming a [0/90] arrangement; Fig. 2(b). The pyramidal truss layers were then snap-fitted into the crosses of the intermediate faces to form the octet-truss lattice; Fig. 2(d). A HYSOL®E-120HP™ (Loctite®Brand, Westlakes, OH) high strength epoxy was finally applied to the nodal regions of the assembled structure. Octet-truss lattice structures were fabricated with a relative density (octahedral cell relative density of the snap-fit lattice) ranging from 1.7 to ~16% by allowing the strut length l, defined in Fig. 2(a), to vary between 8 and 33 mm. All the lattice structures had a strut thickness $t = 1.59$ mm ($t = w$) and node dimensions $b = 4.76$ mm, $c = 2.24$ mm, $h = 0.95$ mm, $h_{tab} = 1.59$ mm, $t_0 = 1.27$ mm, $m = 2.77$ mm, $R = 5.08$ mm, and $\omega = 45°$ (the geometric design variables shown in Fig. 2(a) and (c)). The expression used to calculate the relative density, $\bar{\rho}$ of the snap-fit octahedral cell (Fig. 2(e)) is given in the Supplementary information S.2. Photographs taken at several orientations of the assembled samples are shown in Fig. 3.

In order to predict lattice mechanical properties, the longitudinal and transverse compressive and tensile moduli and strengths of the laminate material were first determined (Supplementary information S.3), and the laminate material was experimentally confirmed to be orthotropic material. Results are shown in Fig. 4(a) and summarized in Table 1. The laminate compressive strengths were different in different loading conditions due to different failure mechanisms: in CLC compression, failure was controlled by plastic fiber micro-buckling, whereas the failure was dominated by delamination in unclamped compression; as observed optically (Fig. 4(c) and (d)) and confirmed by μ−XCT analysis (Fig. 4 (e) and (f)). In both cases, kink bands formed in the plies whose fibers were parallel to the loading direction. The damage modes (kink bands and delamination) were both initiated within the plain weave surface plies where fiber misalignment was the greatest. This initial damage can disturb the subsequent loading condition in unclamped compression by introducing bending moments at the specimen free ends, and stress concentrations can also trigger delamination or matrix cracking near the damage zones prior to plastic fiber micro-buckling of the interior unidirectional plies. In contrast, the CLC test fixture eliminated the end effects, allowing the interior unidirectional plies along the loading direction to fully contribute the plastic fiber micro-buckling strength, and this resulted in a higher compressive strength.

3. Compression responses

The compressive stress−strain responses of the CFRP octet-truss samples are measured (Supplementary information S.4) and shown in Fig. 5(a) and (b). In all cases an initial linear response is observed followed by a regime of nonlinear responses. Typically, the peak stress was attained as strut failure was first observed. The stress then decreased rapidly with increasing strain with serrations on the stress−strain curve associated with a series of strut failures. Photographs of some of the lattice structures after testing are shown in Fig. 5(c)−(g).

The lowest relative density sample ($\bar{\rho} = 1.7\%$) failed by struts Euler buckling. Samples of higher densities failed by delamination of the struts supporting compressive loads. Delamination typically initiated near the ends of the struts and then propagated along the strut axis. During [001] direction free compression, the intermediate faces supported tensile stresses and remained intact after the tests (Fig. 5(c)−(e)) since the tensile strength of the laminate material is much higher than that in compression. During [100]